Design Optimization of A Conventional Rocket Nozzle Using Coupled Thermo-Structural Analysis

M. Dito Saputra[1], Novi Andria[2]

[1,2]Aeroelastics Laboratory, Rocket Technology Center, National Institute of Aeronautics and Space (LAPAN), Indonesia

e-mail: m.dito@lapan.go.id, novi.andria@lapan.go.id

Received: 23-03-2021. Accepted: 29-06-2021 Published: 30-12-2021

Abstract

Thrust in a rocket is gained by expelling combustion gas through a nozzle. Rocket nozzle is a vital component during the conversion of chemical energy into kinetic energy. Consequently, it is exposed to extreme temperature and pressure resulted from gas combustion. Therefore, to ensure a successful rocket operation, the nozzle must be able to maintain structural integrity when being exposed to such environment. On the other hand, its structural weight must be kept minimum to reduce the overall weight of the rocket. Thus, the nozzle design phase is very important since the nozzle significantly affects the whole rocket performance. LAPAN is currently developing some solid-propellant-based rockets. Each rocket's nozzle is still designed using conventional configuration, consists of a metal case and graphite insert, and relies on a thick structure geometry to maintain structural integrity. This approach induces a heavy-weight nozzle that burdens the rocket performance. This paper attempts to optimize LAPAN's conventional solid rocket nozzle design, using RX-450 rocket's nozzle as the studied model. A series of procedures are proposed to generate a lighter nozzle design, with the coupled thermo-structural analysis as the main procedure. The study successfully provided an optimized nozzle geometry with sufficient strength and reduced weight.

Keywords*: solid rocket; nozzle; thermo-structural analysis.*

Nomenclature

E	=	Modulus of Elasticity, GPa	α	=	Coefficient of Thermal Expansion, $10^{-6}/^0$C
T	=	Temperature, ^{0}C	ΔT	=	Temperature Difference, ^{0}C
γ	=	Poisson Ratio	σ	=	Stress, MPa
σ_e	=	Yield Stress, MPa			
k	=	Thermal Conductivity, W/m.K			
C	=	Specific heat, J/Kg.K			
ρ	=	Density, g/cc			
Δx	=	Node Distance, mm			
Δt	=	Time Increment, S			
D	=	Diameter, mm			
s	=	thickness, mm			
A	=	Area, mm^2			
q	=	Heat Flux, mW/mm^2			
P	=	Pressure, Pa			

1. Introduction

Thrust in a solid rocket motor is gained by combusting propellant and discharging the combustion gas result through a supersonic nozzle (Sutton & Biblarz, 2013). Rocket nozzle plays an important role because it acts as an energy converter as it converts the thermal energy in the combustion gas into kinetic energy (Kumar, Nayana, & Shree, 2016). It makes the rocket nozzle exposed to extreme temperature and pressure during the operation periods. The propellant combustion gas result can reach at least 3000 K in temperature or more (Greatrix, 2011). These loads must be taken seriously when designing a rocket nozzle structure since it affects the nozzle structure integrity.

Another factor to be considered during the design phase is the weight as it directly affects the overall rocket performance. A lighter nozzle design requires a lighter balancer or ballast to keep the rocket's center of gravity in the desired location and ultimately reduce the total rocket empty weight.

Heat transfer analysis is a dominant aspect in designing a rocket nozzle structure. Heat in a nozzle structure reduces the material's strength and induces thermal stress. Thermal stress was found to be higher and dominating stress in nozzle structure compared to stress due to mechanical load (Kumar et al., 2005). Mironov (1966) proposed a simplified method for calculating heat transfer in a subsonic and supersonic nozzle. The relative heat transfer equation was used to solve the energy balance. Das, Moore, and Boyer (1988) calculated and compared the heat flux resulting from three modes of heat transfer inside an aluminized solid propellant rocket nozzle which are radiative, convective, and particle impingement. The flow inside the nozzle was calculated using the solid performance computer program [SPP]. Zhang (2011) investigated the transient temperature distribution along a nozzle wall length and thickness. The convective heat transfer is calculated using Bazi equation while the radiative heat transfer is calculated using the radiation in enclosure method. After convective and radiative heat transfer modes have been established, the conductive heat transfer is then solved by using simplified 2D transient conduction in the cylindrical coordinate method.

Banoth (2018) designed a bell-shaped nozzle using GVR Rao's method to define the initial contour of the nozzle. The heat flux along the nozzle's contour is calculated using Bartz equation and the nozzle thickness is determined by comparing the erosion rate of each material that is used with the calculated heat flux. Stress analysis in the nozzle shell is computed using Ansys software. Sun, Bao, Shi, & Xu (2014) performed a coupled fluid, thermal and structural analysis using Ansys software. In the analysis, a frictional coefficient of 0.3 was deployed to observe the effect on the nozzle structural casing. Sun et al. (2016) evaluated the effect of gap existence in a nozzle structure. Thermo structural response of the nozzle structure was carried out using Ansys software and a self-made code made by using Ansys Parameter Design Language (APDL) was deployed to enable coupled thermo-structural analysis. Several gap configurations were observed and compared to find the best fit possible which has the least flame leak risk.

RX-450 is a rocket with a solid propellant and a conventional nozzle type that is currently being developed by the National Institute of Aeronautics and Space (LAPAN), Indonesia. Conventional nozzle in this paper refers to a simple configuration nozzle, consists of graphite insert and metal case. This type of nozzle is suitable for a rocket with a short duration of burning, and it also requires a low cost to manufacture (Sutton & Biblarz, 2013). Currently, RX-450's nozzle uses a thick graphite insert in the convergent up to the throat section while using AISI4340 steel case with no insert in the divergent section. This configuration creates a heavy-weight nozzle due to the thick insert and the thick case that is required in the divergent section.

A series of procedures to optimize RX-450 nozzle design will be proposed in this paper. The aim is to reduce the weight of the nozzle while keeping sufficient strength. The first procedure is to perform heat transfer analysis on a graphite cylinder with an inner contour representing RX-450 nozzle contour. The second procedure is to estimate nozzle case geometry, positioning, and thickness. The estimation was made by considering thermal stress in the insert and the case using previous procedure analysis results as input. The last procedure is to perform a thermo-structure analysis of the proposed nozzle geometry. A thermo-structural analysis consists of heat transfer analysis followed by stress analysis (Kumar et al., 2005). The thermo-structural analysis in this paper was carried out using Patran software to create a finite element model of the nozzle and Marc software to execute analysis calculation. Loads that were used in

this paper are static heat flux and pressure. Temperature-dependent material properties were also utilized to improve analysis results. The thermo-structural analysis results were used to determine the reliability of the proposed nozzle geometry.

Materials used in the optimization attempt are the same as the RX-450 nozzle, which is graphite as insert, and AISI4340 steel as case. No additional material or insulator is added. The manufacturing and assembly aspects are not considered in this paper as the main purpose is to show optimum geometric composition.

This paper is outlined as follows: the material properties and applied load and a brief description of the optimization procedures are discussed in Chapter 2. In Chapter 3, the optimization process is shown, as well with the optimization result and discussion. Finally, the conclusion of this paper is presented in Chapter 4.

2. Methodology

2.1. Materials

Two materials are utilized as the structure of the nozzle in this paper, *i.e.* AISI4340 and graphite. AISI4340 is used as the nozzle case due to its high-strength mechanical properties. AISI4340 is one of the most commonly used steels in aerospace, military, and nuclear industry (Mehrabi, Sharifi, Asadabad, Najafabadi, & Rajaee, 2020). Meanwhile, graphite is used as the nozzle insert since it has a low density and very good thermal properties (Bianchi, Nasuti, Onofri, & Martelli 2011). These features make graphite is very suitable to be used as a part that would be directly exposed to the combustion gas flow.

Most of AISI4340's material properties that are used in this paper are temperature-dependent. The initial value such as modulus of elasticity, yield strength, and Poisson ratio from ASM International (1990) was interpolated using the equation from Gorbănescu & Ancaş (2006). The coefficient of thermal expansion (CTE) is 12.3 µm/m-°C, while the modulus of elasticity was interpolated using Eq. (2-1) and Eq. (2-2) and illustrated in Figure 2-1.

$$\frac{E(T)}{E(20)} = 1 + \frac{T}{2000 \ln\left(\frac{T}{1100}\right)}, 20^0C < T \leq 600^0C \quad (2\text{-}1)$$

$$\frac{E(T)}{E(20)} = \frac{690 - 0.69T}{T - 53.5}, 600^0C < T \leq 1000^0C \quad (1\text{-}2)$$

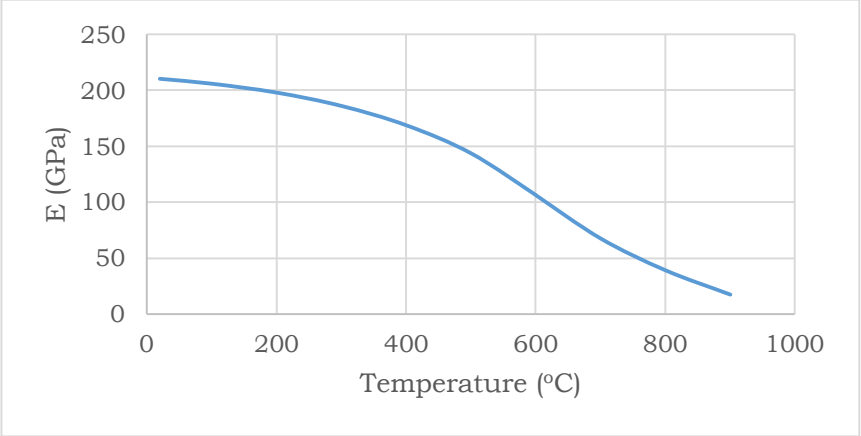

Figure 2-1: Modulus Young of AISI4340 vs. Temperature.

Poisson ratio was interpolated using Eq. (2-3) and Eq. (2-4), as illustrated in Figure 2-2.

$$\gamma(T) = 37.8\ x\ 10^{-5}T + 0.283, 20^0C < T \leq 450^0C \quad (2\text{-}3)$$

$$\gamma(T) = 9.2\ x\ 10^{-5}T + 0.259, T > 450^0C \quad (2\text{-}4)$$

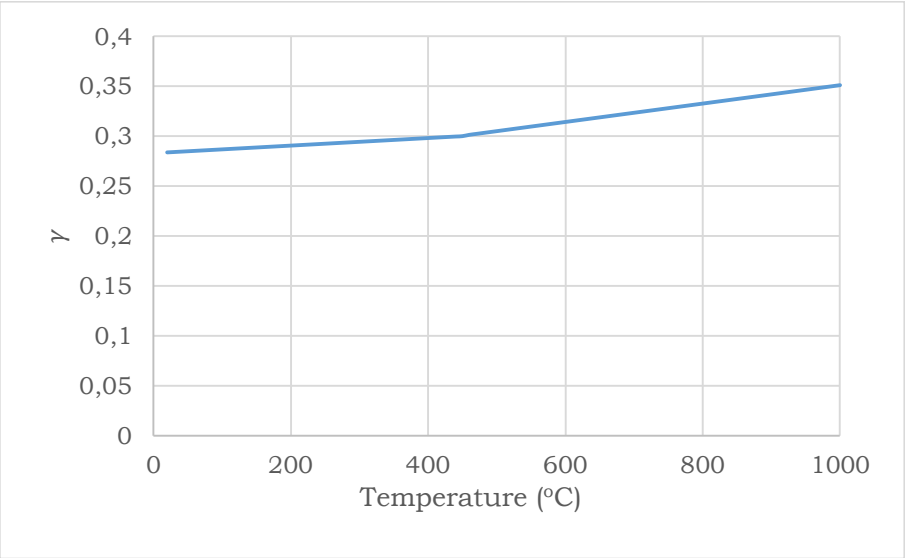

Figure 2-2: Poisson Ratio of AISI4340 vs. Temperature.

Yield stress was interpolated using Eq. (2-5) and Eq. (2-6) and illustrated in Figure 2-3.

$$\frac{\sigma_e(T)}{\sigma_e(20)} = 1 + \frac{T}{900ln\left(\frac{T}{1750}\right)}, 20^0C < T \leq 600^0C \quad (2\text{-}5)$$

$$\frac{\sigma_e(T)}{\sigma_e(20)} = \frac{340 - 0.34T}{T - 240}, 600^0C < T \leq 1000^0C \quad (3\text{-}6)$$

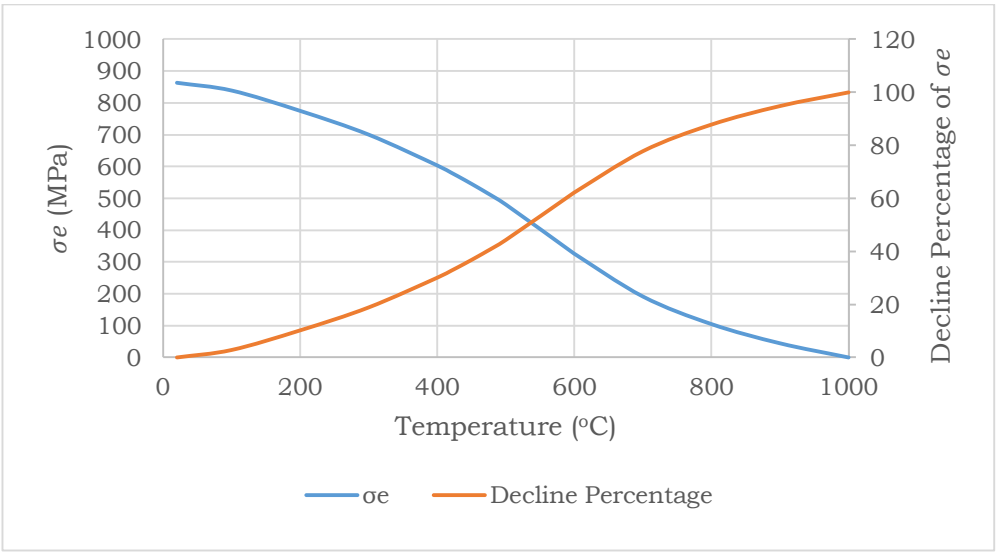

Figure 2-3: Stress Limit and Stress Limit Decline Percentage of AISI4340 vs. Temperature.

For thermal conductivity and specific heat of AISI4340 (Jerniti, Ouafi, & Barka, 2016) illustrated in Figure 2-3.

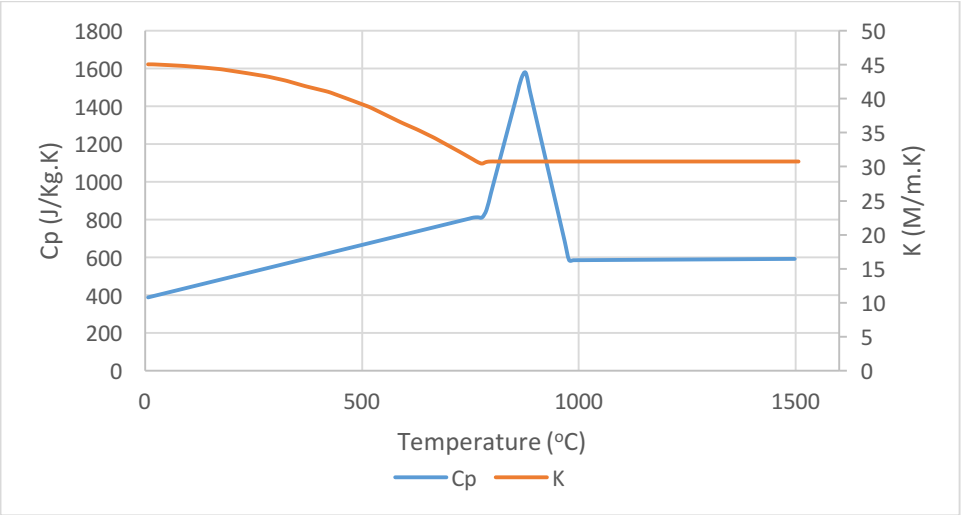

Figure 2-4: Specific Heat and Conductivity of AISI4340 vs. Temperature.

Graphite properties that are used in this paper are as follows: modulus of elasticity of 11,721 GPa, CTE of 8.8 10-6 (in/in)/°C (Entegris, Inc., 2013), Poisson ratio of 0.31, Density of 1,89 g/cc, conductivity of 133 W/m.K, Compressive strength of 136 MPa and conductivity of 726 J/Kg.K (McEligot, Swank, Cottle, & Valentin, 2016).

2.2. Optimization Procedures

The RX-450 nozzle's design optimization in this paper begins with a heat transfer analysis in a graphite cylinder with a cavity following RX-450 nozzle's contour. The nozzle contour can be seen in Figure 2-5.

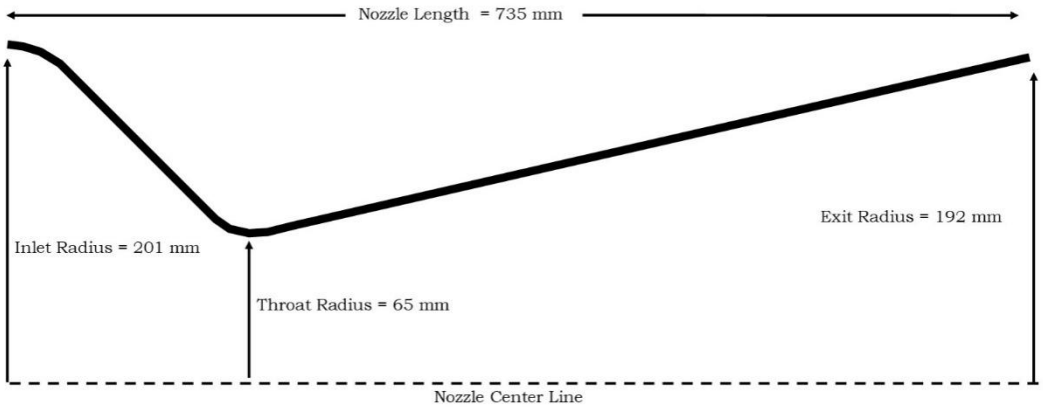

Figure 2-5: The Internal Contour of RX-450 Nozzle.

The following procedure is to estimate the nozzle's case contour and thickness. The case's contour and thickness were determined by using graphite heat distribution results as input. Estimation is made by considering thermal stress induced by temperature gradient in the insert and the case. Thermal stress in the case must not exceed the yield strength of the material at the corresponding temperature. At the same time, thermal stress in the insert is to be kept as low as possible to minimize the damage to the nozzle insert. Estimation is made by collecting nodal temperature output in several directions following the nozzle's inner contour. The directions to be followed are represented by several lines, which are lines A, B, C, and D, as shown in Figure 2-6. The dimensional constraint of the case is the outside radius must not exceed 226.25 mm.

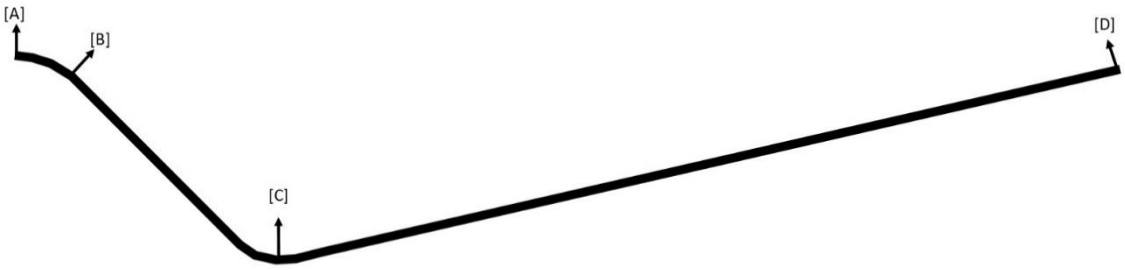

Figure 2-6: Nozzle Case Estimation Direction.

Once the case location and thickness have been determined as the second step procedure is accomplished, the last step can be performed. The final step is to perform a thermo-structural analysis on the proposed nozzle geometry to verify the structural integrity.

2.3. Loads

Two loads were applied in this paper to represent the nozzle operational environment condition. The loads are heat flux and pressure. Both loads were applied for 12 seconds corresponding to the RX-450 burn time. The pressure load is shown in Figure 2-7.

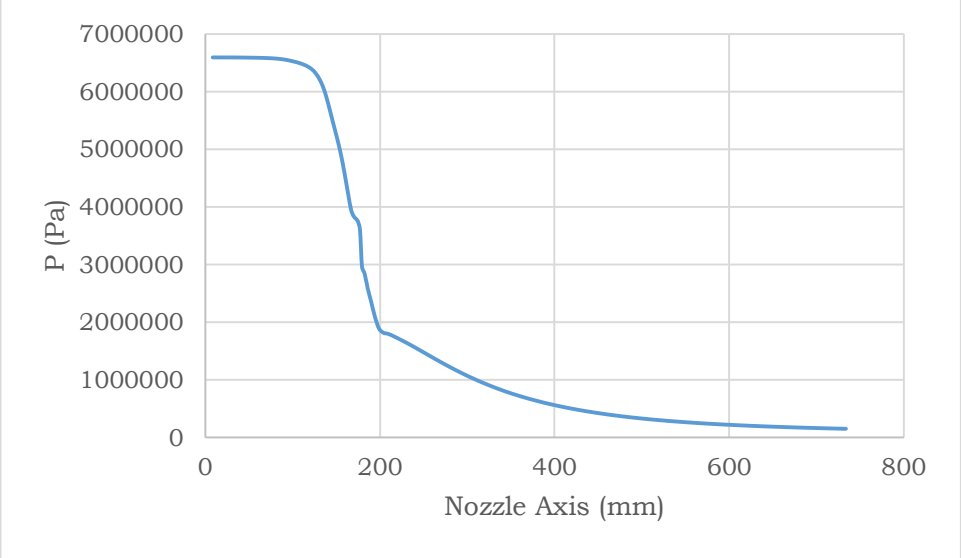

Figure 2-7: Pressure Load Along Nozzle Axis.

And the heat flux load is shown in Figure 2-8.

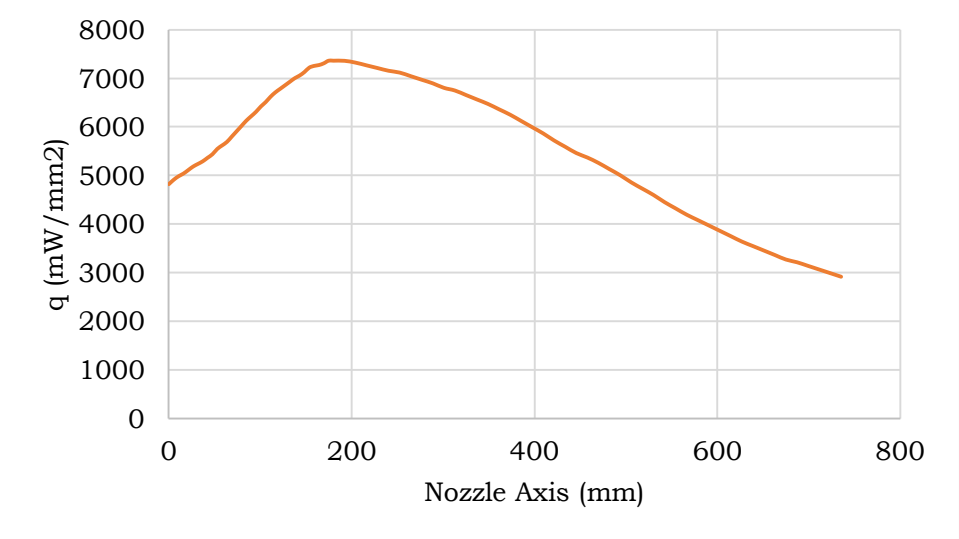

Figure 2-8: Heat Flux Load Along Nozzle Axis.

3. Result and Analysis

The first process in the design procedure is to perform an initial transient thermal analysis on a graphite cylinder model as shown in Figure 3-1. The inner cavity's contour of the model represents the RX-450's nozzle contour (Figure 2-5), while the outer radius is 226.25 mm. The graphite cylinder was discretized using hex8 element type with 4 mm length. The outcome of this step is transient temperature distribution within the graphite cylinder. It was used as input for the nozzle's case thickness estimation in the next design step.

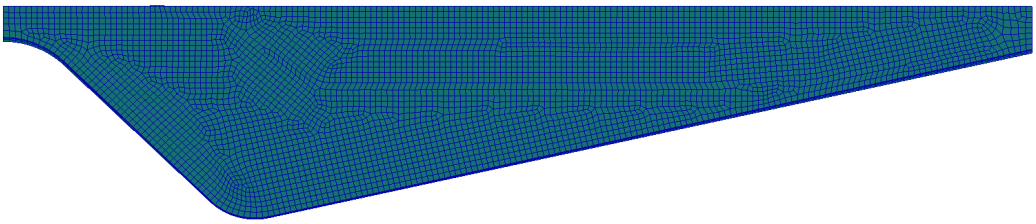

Figure 3-1: Finite Element Model of Graphite Cylinder.

The load that was applied in this analysis step is the heat flux load (Figure 2-8). The heat flux was applied for the entire duration of the rocket burning time, which is 12 seconds. The analysis was done using a transient thermal analysis module in Marc software. The heat transfer analysis result of the graphite cylinder is shown in Figure 3-2.

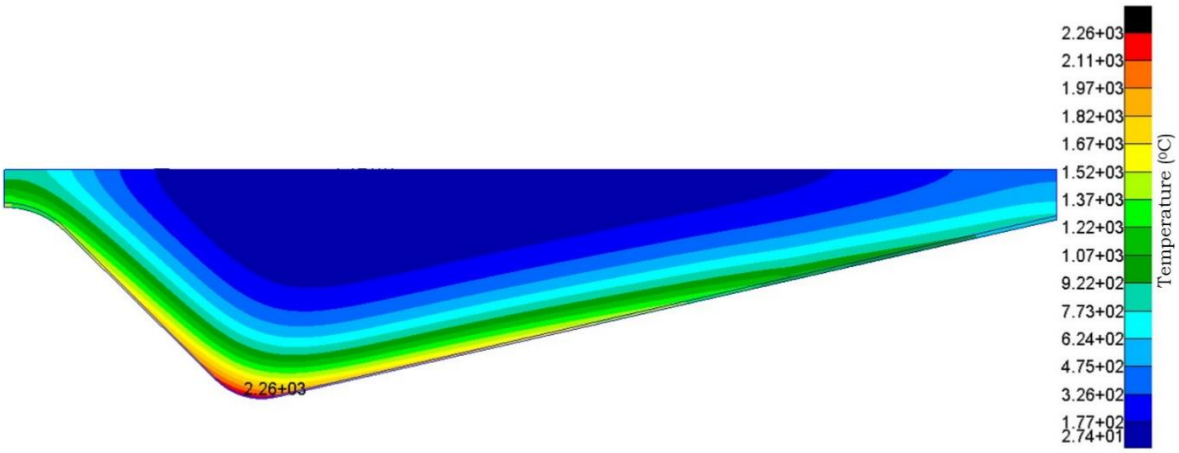

Figure 3-2: Graphite Cylinder Heat Transfer Result at t=12 Second.

Nozzle case was then designed by determining the nearest safe location for the case from the nozzle inner contour. A near-safe location means a smaller case inner radius thus reduces the volume of the nozzle insert which reduces the nozzle weight. It also decreases the temperature difference between the inner and the outer surface of the insert which leads to lower thermal stress induced in the insert. Case location determination would also consider the thermal stress induced to the case and the material's temperature dependant properties. Thermal stress was then calculated using Eq. (3-1) (Irfan & Chapman, 2009).

$$\sigma = 1.25\frac{\alpha E \Delta T}{2(1-\gamma)} \tag{3-1}$$

To determine the temperature difference between the case's surfaces, a 1D transient finite difference method was used. This estimation method is considered to be reliable even though the geometric shape is cylinder due to the case's diameter and thickness ratio value is expected to exceed 10 (D/s >10), thus the case can be treated as a flat plate (Jaremkiewicz & Taler, 2020). As the input for the estimation, each nodal transient temperature result from the graphite cylinder heat transfer analysis (Figure 3-2) along

the nozzle case estimation direction line (Figure 2-6) was calculated. To calculate the temperature difference between the case's surfaces, Eq. (3-2) was used (Cengel, 1995).

$$kA\frac{T_{m-1}-T_m}{\Delta x}+kA\frac{T_{m+1}-T_m}{\Delta x}=\rho AC\Delta x\frac{T_m^{i+1}-T_m^i}{\Delta t} \quad (3\text{-}2)$$

Due to the extreme heat in the throat section, it is impossible to keep the thermal stress of all portions of the insert in the throat section below the graphite's strength limit. Some trade-off has to be made to maintain the case's integrity since extreme temperature degrades the case's material strength. Another aspect is to keep the temperature difference in the case minimum to reduce thermal stress in the case. These considerations resulting in a small portion of the insert in the throat section will degrade due to high stress.

After performing nozzle case location estimation using Eq. (3-1) and Eq. (3-2) using nodal transient temperature result (Figure 3-2) as input along the estimation line (Figure 2-6). Nozzle case geometric shape was drawn at each nodal location which yields the lowest thermal stress. The geometric result of the nozzle is shown in Figure 3-3.

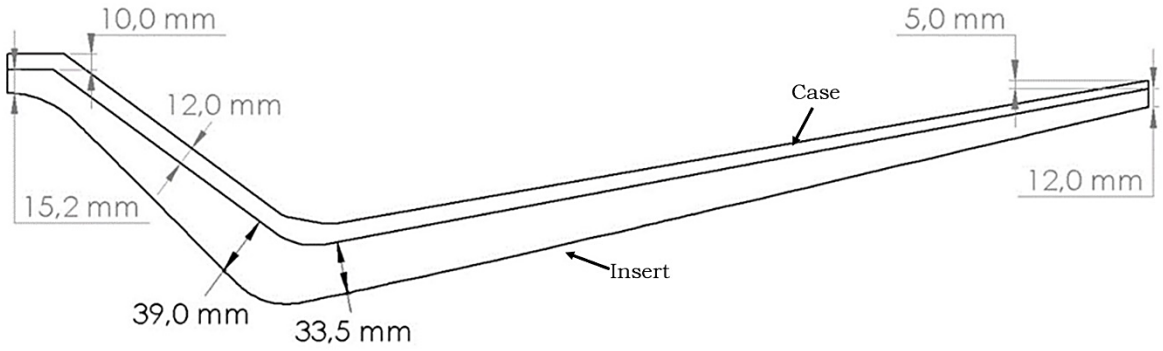

Figure 3-3: Nozzle Case and Insert Geometry.

The proposed nozzle design weight is about 87.7 kg, which is 40% lighter than the current RX-450 nozzle design. Once the nozzle geometric has been decided, thermo-structural analysis is performed on the proposed nozzle geometry. Pressure (Figure 2-7) and heat flux load (Figure 2-8) were applied at the inner surface of the nozzle. Transient coupled thermo-structural analysis mode in Marc software was used to analyze the temperature and stress distribution along the nozzle case thickness and length. The temperature distribution result at the 12th second in the overall nozzle structure is shown in Figure 3-4.

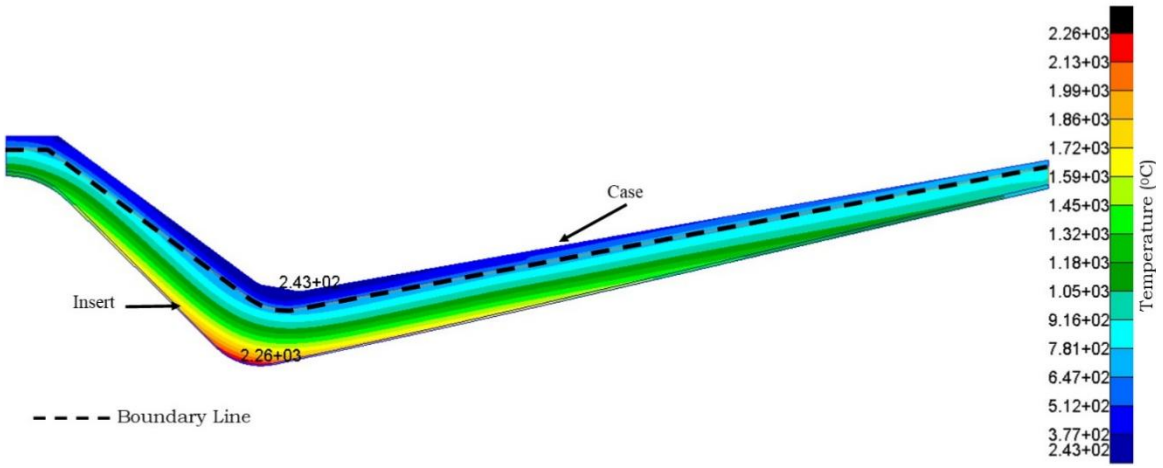

Figure 3-4: Overall Temperature Distribution.

Meanwhile, the temperature distribution at 12th second in nozzle case alone is shown in Figure 3-5.

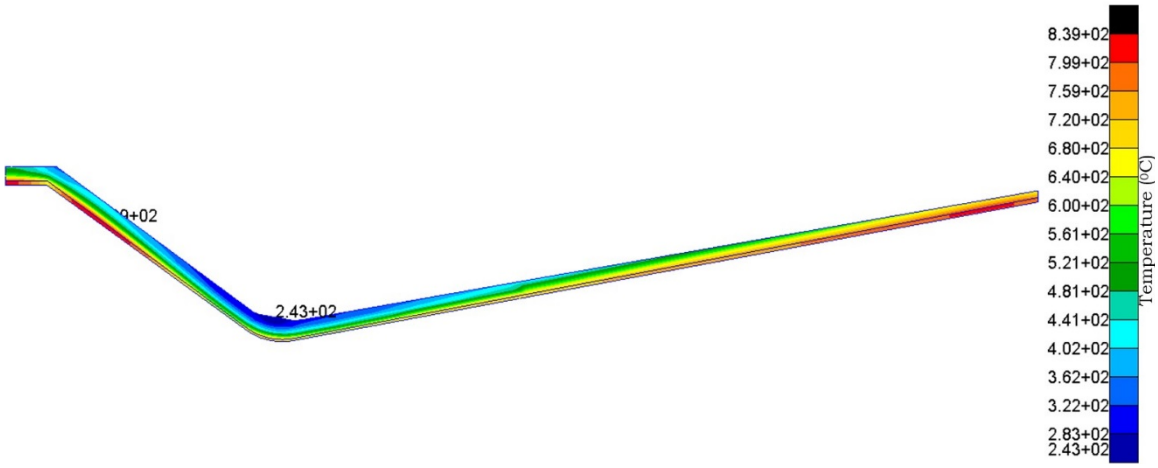

Figure 3-5: Nozzle Case Temperature Distribution.

A detail of temperature distribution at the 12th second on the outer case surface is shown in Figure 3-6.

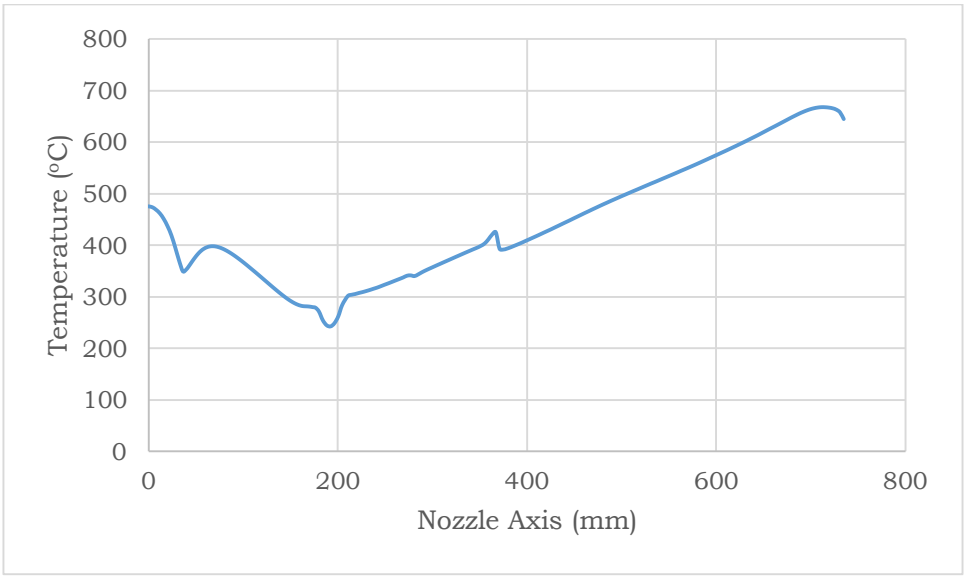

Figure 3-6: Nozzle Case Outer Surface Detail Temperature Distribution.

Stress distribution at the 12th second of the nozzle case is shown in Figure 3-7.

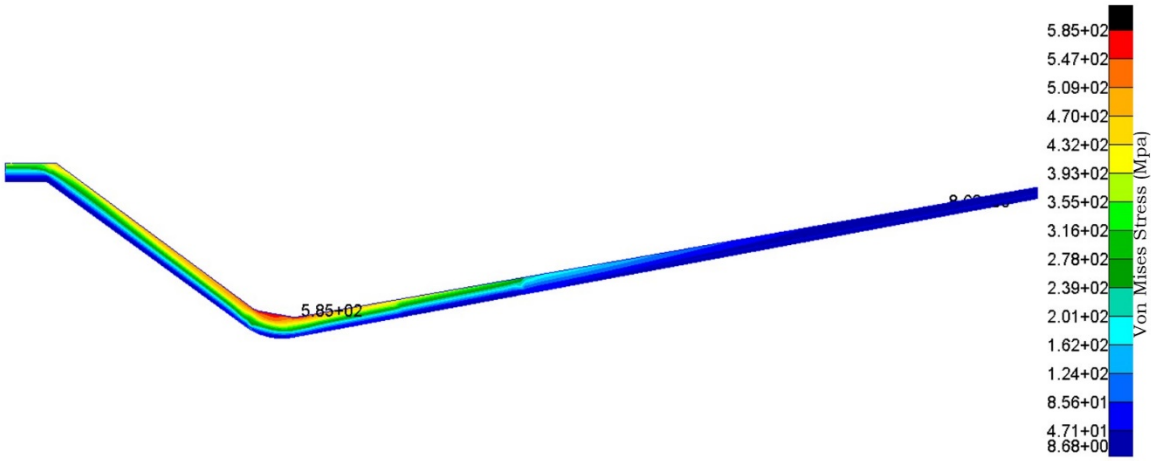

Figure 3-7: Nozzle Case Outer Surface Stress Distribution.

Detail of Von Mises stress distribution at the 12th second on the outer and inner surface of the case is shown in Figure 3-8.

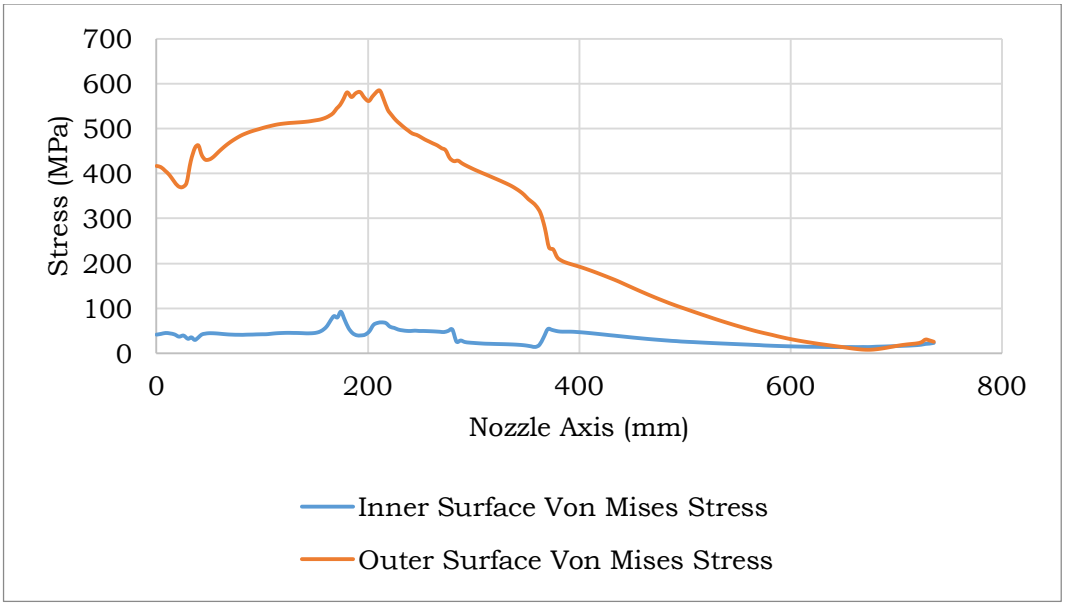

Figure 3-8: Nozzle Case Surfaces Stress Distribution.

After acquiring the total stress distribution in both surfaces of the nozzle case, we could evaluate the nozzle case safety factor by finding the ratio between each nodal stress distribution with the corresponding AISI 4340 yield strength at each nodal temperature (Figure 2-3). The safety factor along the nozzle axis can be seen in Figure 3-9.

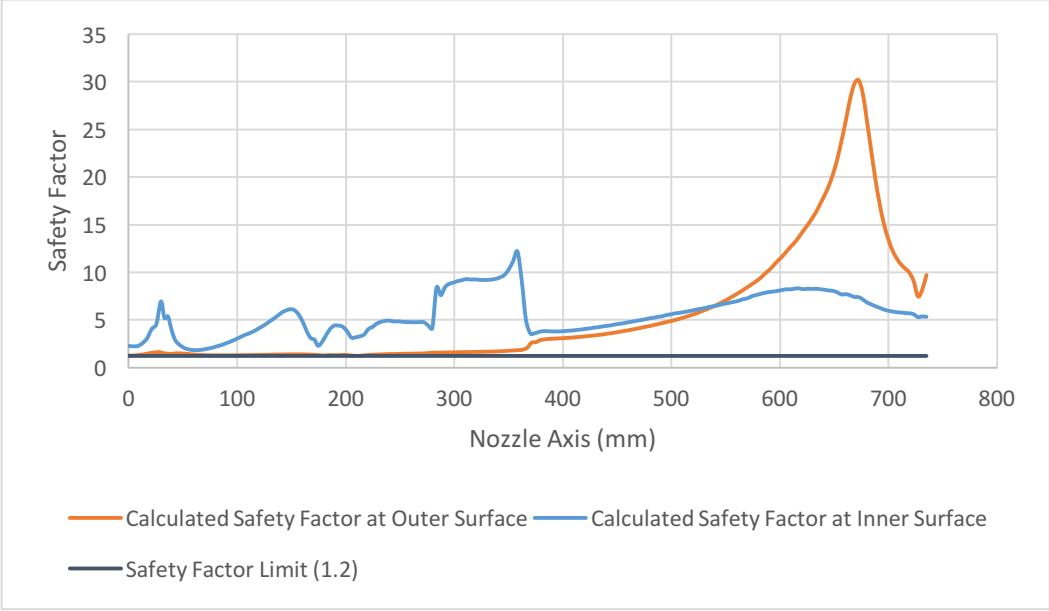

Figure 3-9: Nozzle Case Safety Factor.

From Figure 3-9, we could understand that all area on the outer and inner surface of the case exhibits a sufficient level of safety (safety factor ≥ 1.2). The area with the lowest safety factor is the outer surface of the case between axis 0-360 mm. The level of safety factor in the area is caused by the high heat flux and pressure load. It could be seen from Figure 3-7 that the Von Mises stress results are spiking the area. The safety factor value could be improved by moving the case outward, but it will increase the nozzle weight and the thermal stress in the insert's inner surface. The inner surface of the case

experienced a relatively high safety factor across the nozzle axis. By using these considerations, the proposed nozzle geometry can be considered reliable.

4. Conclusions

This paper has presented a procedure to optimize the design of a conventional rocket nozzle. The research that has been done shows that the proposed procedure is applicable in optimizing RX-450 rocket nozzle's design as the studied object. The proposed nozzle geometry shows about 40% mass reduction and can withstand the RX-450 rocket nozzle operational environment at the same time. This research's analysis shows that the nozzle case's stress distribution is still within the safe limit across the nozzle axis.

Future development may be done by developing a program that could bridge the Patran and Marc software. The program's purpose is to allow two-way feedback between the software so continuous iterative thermocouple analysis could be established. The iteration is set to find the lightest geometry configuration within the desired safety factor limit with the specified geometrical constraint and operational loads.

Acknowledgements

The authors express gratitude for the support of the Head of the Rocket Technology Center–Indonesian National Institute of Aeronautics and Space (LAPAN).

Contributorship Statement

MDS developed the simulation and prepared the manuscript; NA took the role of mentor and supervisor.

References

ASM International. (1990). *ASM handbook volume 1*: *Properties and selection: Irons, steels, and high-performance alloys*. Materials Park, OH: Author. https://doi.org/https://doi.org/10.31399/asm.hb.v01.9781627081610

Banoth, M. (2018). Structural analysis of rocket nozzle. *International Journal of Science and Research (IJSR)*, *7*(7), 300–313. https://doi.org/10.21275/ART20183795

Bianchi, D., Nasuti, F., Onofri, M., & Martelli, E. (2011). Thermochemical erosion analysis for graphite/carbon–carbon rocket nozzles. *Journal of Propulsion and Power*, *27*(1), 197–205. https://doi.org/10.2514/1.47754

Cengel, Y. A. (1995). *Heat transfer: A practical approach* (2nd ed.). New York City, NY: McGraw-Hill.

Das, D. K., Moore, G. R., & Boyer, C. T. (1988). Heat transfer studies on a rocket nozzle for naval application. *Naval Engineers Journal*, *100*(1), 29–35. https://doi.org/10.1111/j.1559-3584.1988.tb01450.x

Entegris, Inc. (2013). *Properties and characteristics of graphite* [Brochure]. Billerica, MA: Author.

Gorbănescu, D. & Ancaş, A. (2006). Theoretical models in the study of temperature effect on steel mechanical properties. *Bulletin of the Polytechnic Institute of Jassy: Constructions, Architecture Section, LII(LVI)*(1–2), 49–54.

Greatrix, D. R. (2011). Scale effects on solid rocket combustion instability behaviour. *Energies*, *4*(1), 90–107. https://doi.org/10.3390/en4010090

Irfan, M. A. & Chapman, W. (2009). Thermal stresses in radiant tubes due to axial, circumferential and radial temperature distributions. *Applied Thermal Engineering*, *29*(10), 1913–1920. https://doi.org/10.1016/j.applthermaleng.2008.08.021

Jaremkiewicz, M. & Taler, J. (2020). Online determining heat transfer coefficient for monitoring transient thermal stresses. *Energies*, *13*(3). https://doi.org/10.3390/en13030704

Jerniti, A. G., Ouafi, A. El, & Barka, N. (2016). Single track laser surface hardening model for AISI 4340 steel using the finite element method. *Modeling and Numerical Simulation of Material Science*, *06*(02), 17–27. https://doi.org/10.4236/mnsms.2016.62003

Kumar B, D., Nayana, S. B., & Shree, D. S. (2016). Design and structural analysis of

solid rocket motor casing hardware used in aerospace applications. *Journal of Aeronautics & Aerospace Engineering*, *5*(2). https://doi.org/10.4172/2168-9792.1000166

Kumar, R. R., Vinod, G., Renjith, S., Rajeev, G., Jana, M. K., & Harikrishnan, R. (2005). Thermo-structural analysis of composite structures. *Materials Science and Engineering A*, *412*(1–2), 66–70. https://doi.org/10.1016/j.msea.2005.08.065

McEligot, D. M., Swank, W. D., Cottle, D. L., & Valentin, F. I. (2016). *Thermal properties of G-348 graphite*. https://www.osti.gov/servlets/purl/1330693

Mehrabi, A., Sharifi, H., Asadabad, M. A., Najafabadi, R. A., & Rajaee, A. (2020). Improvement of AISI 4340 steel properties by intermediate quenching – microstructure, mechanical properties, and fractography. *International Journal of Materials Research (Formerly Zeitschrift Fuer Metallkunde)*, *111*, 771–779. https://doi.org/10.3139/146.111939

Mironov, B. P. (1966). Calculation of heat transfer in nozzles. *Journal of Applied Mechanics and Technical Physics*, *7*(4), 83–86. https://doi.org/10.1007/BF00917667

Sun, L., Bao, F., Shi, W., & Xu, H. (2014). Coupled fluid, thermal and structural analysis of nozzle in solid rocket motor. *Applied Mechanics and Materials*, *482*, 297–301. https://doi.org/10.4028/www.scientific.net/AMM.482.297

Sun, L., Bao, F., Zhang, N., Hui, W., Wang, S., Zhang, N., & Deng, H. (2016). Thermo-structural response caused by structure gap and gap design for solid rocket motor nozzles. *Energies*, *9*(6). https://doi.org/10.3390/en9060430

Sutton, G. P. & Biblarz, O. (2013). *Rocket propulsion elements* (7th ed.). Hoboken, NJ: John Wiley & Sons.

Zhang, X. (2011). Coupled simulation of heat transfer and temperature of the composite rocket nozzle wall. *Aerospace Science and Technology*, *15*(5), 402–408. https://doi.org/10.1016/j.ast.2010.09.006